International Journal of Latest Trends in Engineering and Technology
Vol.(22)Issue(4), pp.001-009
DOI: http://dx.doi.org/10.21172/1.224.01
e-ISSN:2278-621X

DYNAMIC ANALYSIS ON BUILDINGS FITTED WITH VISCOUS FLUID DAMPERS USING A GENERAL APPROACH

Pham Nhan Hoa[1]

Abstract- **This paper introduces a General Approach model and an associated numerical method with its algorithm to examine the seismic responses of a structure fitted with viscous fluid dampers (VFD) under dynamic loads. This method considers the stiffness matrix of the beam, leading to a reduction in the lateral frame's stiffness matrix value. The numerical examples used are steel structures facing benchmark problems, subjected to a horizontal seismic load to present comparative response results in scenarios including the Shear Frame model (SF), General Approach model (GA), and Finite Element model (FE). A ratio is introduced that compares the flexural stiffness of the beam to that of the column to estimate the change from GA modal to SF modal. The conclusions drawn from these examples offer a more precise evaluation of response reduction for such a building.**

Keywords – Structural Control, Dynamics of Structures, Viscous Fluid Dampers, General Approach, Smart structures

I. INTRODUCTION

Structural control mechanisms for buildings fitted with dissipators have been evolving for quite some time and can be divided into three categories [8]: passive, semi-active, and active controls. Recently, structures using passive Viscous Fluid Dampers (VFD) have been developed [4][5][6][7], as VFDs significantly reduce the dynamic response of the building. However, these papers analyze the dynamic behaviors of a structure with VFDs using the shear frame model (SF), which assumes that the beams of a structure are perfectly rigid, with infinite axial and flexural stiffness. This assumption stems from viewing the slab and beam at each floor of a building as a dependent mass. As a result, SF is not suitable for large span structures. To address this issue, the General Approach model (GA) is introduced [2], which disregards axial deformation in both beams and columns and neglects shear deformation in beams. In GA, the columns of each story still have the same lateral displacement (Fig. 2), while the beams' flexural stiffness, which contributes to the lateral stiffness of a structure, is still considered. Furthermore, GA uses fewer degrees of freedom than FEM, which is beneficial for analyzing soil-structure interaction problems that require substantial resources to represent building motion for computation. Ultimately, the dynamic responses of a structure retrofitted with VFDs using GA provide a more thoughtful evaluation of the effectiveness of VFDs in reducing response. This finding also lays the groundwork for further research on structures equipped with various types of dissipators, including friction dampers, variable stiffness dampers, and Magneto Rheological Dampers.

[1] *School of Civil Engineering and Management, International University - VNU HCM, Ho Chi Minh City, Vietnam*
Vietnam National University, Ho Chi Minh City, Vietnam

II. The Differential Equation Governing the Motion of a Structure Equipped with VFD using General Approach

II.1. Computational Model

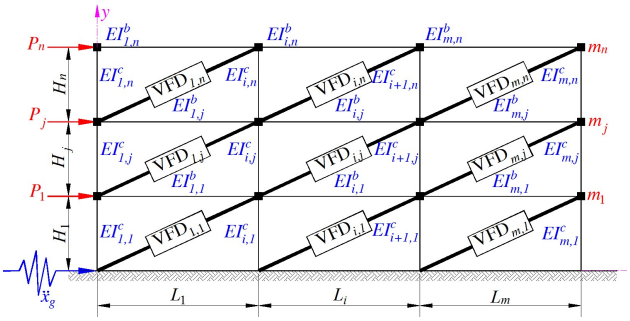

Fig. 1: Mathematical model of a structure retrofitted with VFD subjected to external dynamic forces

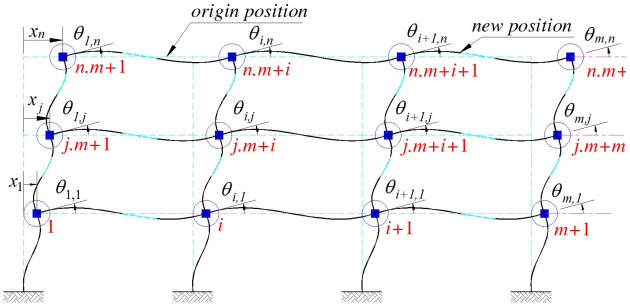

Fig. 2. Degrees of freedom (DOFs) of a structure

Consider the *m*-bay, *n*-story planar two-dimensional frame shown in Fig. 1. The structure is equipped with *m*×*n* VFDs at each of the portals. The excitation consists of lateral forces P_i at the *n* floor levels $\left(i=\overline{1,m}\right)$ and horizontal ground motion $\ddot{x}_g$ due to an earthquake. The story height is $H_j\left(j=\overline{1,n}\right)$ and the bay width L_i. The flexural rigidities of uniform beams and columns are $EI^b_{i,j}$ and $EI^c_{i,j}$ respectively; m_j is the total mass of the j^{th} level. In Finite Element model [1] a node in 2D frame has three DOFs including two translations (*x,y* components) and one rotations (about *z* axis). For simple and on purpose of neglecting the axial deformation in the columns and beams of a frame, the General Approach [2] is introduced. It is a *m*-bay, *n*-story frame having *n*×(*m*+1) nodes and *n*×(*m*+2) DOFs (Fig. 2). For beam and column elements, their deformations are illustrated in Fig.3 and Fig. 4. Consequently, their internal element forces including bending moments and shears at the ends.

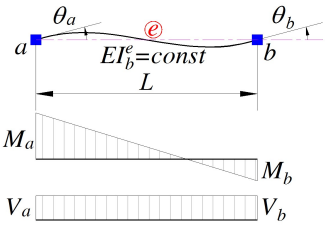

Fig. 3: A typical uniform beam element

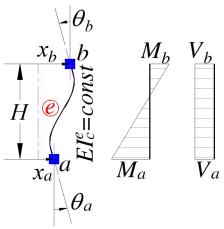

Fig. 4. A typical uniform column element

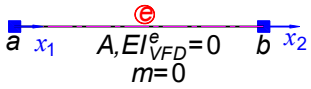

Fig. 5. a VFD element

for beam,
$$\begin{cases} V_a=\dfrac{6EI}{L^2}\left(\theta_a+\theta_b\right) \\ V_b=-\dfrac{6EI}{L^2}\left(\theta_a+\theta_b\right)=-V_a \\ M_a=\dfrac{2EI}{L}\left(2\theta_a+\theta_b\right) \\ M_b=\dfrac{2EI}{L}\left(\theta_a+2\theta_b\right) \end{cases} \quad (1)$$
and for columns,
$$\begin{cases} V_a=\dfrac{2EI}{H^3}\left[6\left(u_a-u_b\right)-3H\left(\theta_a+\theta_b\right)\right] \\ V_b=\dfrac{2EI}{H^3}\left[-6\left(u_a-u_b\right)+3H\left(\theta_a+\theta_b\right)\right] \\ M_a=\dfrac{2EI}{H^2}\left[-3\left(u_a-u_b\right)+H\left(2\theta_a+\theta_b\right)\right] \\ M_b=\dfrac{2EI}{H^2}\left[-3\left(u_a-u_b\right)+H\left(\theta_a+2\theta_b\right)\right] \end{cases} \quad (2)$$

Using the beams and columns' internal forces in this static equilibrium, the stiffness matrices in a typical beam element (with respect to the displacement vector $\{u_1,u_2\}^T=\{\theta_a,\theta_b\}^T$) and column element (with respect to the displacement vector $\{u_1,u_2,u_3,u_4\}^T=\{u_a,u_b,\theta_a,\theta_b\}^T$) are respectively written as

$$\mathbf{K_b^e}=\frac{2EI_b^e}{L}\begin{bmatrix}2 & 1\\ sym & 2\end{bmatrix} \quad (3); \qquad \mathbf{K_c^e}=\frac{2EI_c^e}{H^3}\begin{bmatrix}6 & -6 & -3H & -3H\\ & 6 & 3H & 3H\\ & & 2H^2 & H^2\\ sym & & & 2H^2\end{bmatrix} \quad (4)$$

In shear frame model of a structure, a displacement vector is only two transverse displacements and therefore its corresponding stiffness matrix is $\left(\mathbf{K_c^e}\right)_{\mathbf{SF}} = \dfrac{12EI_c^e}{H^3}\begin{bmatrix} 1 & -1 \\ sym & 1 \end{bmatrix}$ (5)

Labeling global DOFs as $\left\{u_1, u_2, ..., u_{n\times(m+2)}\right\}^T = \left\{x_1, x_2, ..., x_n, \theta_{1,1}, \theta_{2,1}, ..., \theta_{n(m+1)}\right\}^T$ lead to a global stiffness matrix by $\mathbf{K} = \left[\begin{array}{c|c} \mathbf{K}_{n\times n} & \mathbf{K}_{n\times n(m+1)} \\ \hline \mathbf{K}_{n(m+1)\times n} & \mathbf{K}_{n(m+1)\times n(m+1)} \end{array}\right]$ (6) where $\mathbf{K}_{n\times n}$ - a stiffness matrix involving transverse displacements, $\mathbf{K}_{n(m+1)\times n(m+1)}$ - a stiffness matrix related to rotation displacements, $\mathbf{K}_{n\times n(m+1)}$ and $\mathbf{K}_{n(m+1)\times n}$ - the stiffness matrix considering the effect of transverse displacements on rotational displacements and vice versa. The subscripts denote their dimensions.

A global mass matrix of the structure can be determined by one of the two procedures [2]

① *Ignoring the rotational inertia* (or the pure transverse inertia), the lumped-mass element matrix of a beam is reduced as $\mathbf{M_b^e} = \begin{bmatrix} 0 & 0 \\ 0 & 0 \end{bmatrix}$ (7) in which m_a and m_b are the concentrated masses of a beam element at its ends *a* and *b*.

For a beam at the j^{th} story, its m_a and m_b are calculated as $m_a^e = m_b^e = \dfrac{m_j}{\sum_{i=1}^{m} L_i}\dfrac{L^e}{2}$. Although the rotational inertia of a beam is not taken into account, $\mathbf{M_b^e}$ is existed as a result of a global mass matrix assembly, and the consistent-mass element matrix of a column (with respect to $\left\{u_1, u_2\right\}^T = \left\{u_a, u_b\right\}^T$) is reduced as $\mathbf{M_c^e} = \dfrac{m_c^e L}{420}\begin{bmatrix} 156 & 54 \\ sym & 156 \end{bmatrix}$ (8) where m_c^e - distributed mass in a column element.

And then assemble column's mass matrices into the global mass matrix which can be written in the matrix form as $\mathbf{M_{lumped}} = \left[\begin{array}{c|c} \mathbf{M}_{n\times n} & \mathbf{0}_{n\times(m+1)} \\ \hline \mathbf{0}_{(m+1)\times n} & \mathbf{0}_{n(m+1)\times n(m+1)} \end{array}\right]$ (9) where $\mathbf{0}_{n\times(m+1)}$, $\mathbf{0}_{(m+1)\times n}$, and $\mathbf{0}_{n(m+1)\times n(m+1)}$ are zero matrices.

$\mathbf{M}_{n\times n} = \begin{bmatrix} m_1 & & & & \\ & \ddots & & & \\ & & m_j & & \\ & & & \ddots & \\ & & & & m_n \end{bmatrix}$ (10) is a diagonal matrix.

② *Allowing for the rotational inertia* of beams and columns, the beam and column consistent mass matrices are taken as $\mathbf{M_b^e} = \dfrac{m_b^e L^3}{420}\begin{bmatrix} 4 & -3 \\ sym & 4 \end{bmatrix}$ (11) ; $\mathbf{M_c^e} = \dfrac{m_c^e H}{420}\begin{bmatrix} 156 & 54 & -22H & 13H \\ & 156 & -13H & 22H \\ & & 4H^2 & -3H^2 \\ sym & & & 4H^2 \end{bmatrix}$ (12) with $m_{b/c}^e$ - distributed mass in a beam/column element; and subsequently assemble the element mass matrices into the global consistent mass matrix which can be written in the matrix form as $\mathbf{M_{consistent}} = \left[\begin{array}{c|c} \mathbf{M}_{n\times n} & \mathbf{0}_{n\times(m+1)} \\ \hline \mathbf{0}_{(m+1)\times n} & \mathbf{M}_{n(m+1)\times n(m+1)} \end{array}\right]$ (13) in which $\mathbf{M}_{n(m+1)\times n(m+1)}$ is a mass matrix indicating rotational inertia and evaluated by element's mass matrices due to rotation at nodes.

The differential equation governing the motion of the structure is expressed in the form as $\mathbf{M\ddot{u} + C\dot{u} + Ku = P - M_{lumped}}\,\mathbf{1}\ddot{u}_g - \mathbf{F_{VFD}}$ (14) where the mass matrix $\mathbf{M}$ is either $\mathbf{M_{lumped}}$ or $\mathbf{M_{consitent}}$; $\mathbf{C}$ – the damping matrix of the structure computed by using the Raleigh damping fomula as [2]; $\mathbf{C} = a_0\mathbf{M} + a_1\mathbf{K}$ with $a_0 = \dfrac{2\omega_i\omega_j\left(\omega_i\zeta_i - \omega_j\zeta_j\right)}{\omega_i^2 - \omega_j^2}$ and $a_1 = \dfrac{2\left(\omega_i\zeta_i - \omega_j\zeta_j\right)}{\omega_i^2 - \omega_j^2}$ (15) where the coefficients a_0 and a_1 are functions of damping

ratios ζ_i and ζ_j for the i^{th} and j^{th} modes. Obviously this linear damping matrix $\mathbf{C}$ has the same matrix form of $\mathbf{K}$ and $\mathbf{M}$ as $\mathbf{C}=\begin{bmatrix}\mathbf{C}_{n\times n} & \mathbf{C}_{n\times n(m+1)}\\ \mathbf{C}_{n(m+1)\times n} & \mathbf{C}_{n(m+1)\times n(m+1)}\end{bmatrix}$; $\mathbf{u}=\begin{Bmatrix}\mathbf{x}_{n\times 1}\\ \boldsymbol{\theta}_{n(m+1)\times 1}\end{Bmatrix}$ - displacement vector containing lateral displacements $\mathbf{x}_{n\times 1}$ at the levels and rotation displacements $\boldsymbol{\theta}_{n(m+1)\times 1}$ at the nodes; $\dot{\mathbf{u}}=\frac{d}{dt}\mathbf{u}$ and $\ddot{\mathbf{u}}=\frac{d^2}{dt^2}\mathbf{u}$ - velocity and acceleration vectors; $\mathbf{P}=\left[P_1,...,P_i,...,P_{n(m+2)}\right]^T$ - externally forces; $1=\begin{bmatrix}\mathbf{1}_{n\times 1} & \mathbf{0}_{n\times 1}\\ \mathbf{0}_{n(m+1)\times 1} & \mathbf{1}_{n(m+1)\times 1}\end{bmatrix}$ - a diagonal matrix with $\mathbf{1}_{n\times 1}=\left[1,...,1,...,1\right]^T$; $\ddot{\mathbf{u}}_{\mathbf{g}}=\begin{Bmatrix}\ddot{x}_g\\ \ddot{\theta}_g\end{Bmatrix}$ - ground acceleration; a force vector generated by VFD as $\mathbf{F}_{\mathbf{VFD}}=\begin{Bmatrix}\mathbf{F}^{\mathbf{VFD}}_{n\times 1}\\ \mathbf{0}_{n(m+1)\times 1}\end{Bmatrix}^T$ (16)

where $\mathbf{F}^{\mathbf{VFD}}_{n\times 1}=\left\{F_1^{VFD}-F_2^{VFD},...,F_j^{VFD}-F_{j+1}^{VFD},...,F_n^{VFD}\right\}^T$ in which $F_j^{VFD}\left(j=\overline{1,n}\right)$ is a horizontal total force in VFD at the j^{th} story and determined as $-F_j^{\max}\le F_j^{VFD}=C_j^{VFD}\left|\dot{x}_j-\dot{x}_{j-1}\right|^{\alpha_j}\operatorname{sign}\left(\dot{x}_j-\dot{x}_{j-1}\right)\le F_j^{\max}$ (17) with $C_j^{VFD}=\sum_{i=1}^{m}C_{i,j}$ and $\alpha_j=\left[0.5\div 1.2\right]$ are coefficients and set up VFD in advance; $\left(\dot{x}_j-\dot{x}_{j-1}\right)$ is interstory velocity; and F_j^{VFD} is the damper force at the j^{th} story. This value does not exceed the maximum damper force $F_j^{\max}$, a value obtainable from VFD manufactors.

The dynamics internal forces of a beam element are caused by rotational dynamic responses at its two ends including displacements, velocities, and accelerations determined as $\mathbf{F_e}=\mathbf{M_e}\ddot{\mathbf{u}}_\mathbf{e}+\mathbf{C_e}\dot{\mathbf{u}}_\mathbf{e}+\mathbf{K_e}\mathbf{u_e}$ (18) where the value of $\mathbf{M_e}$ depends on either ignoring or allowing for the rotational inertia.

For instant, *neglecting the rotational inertia*, its shear forces and moments at the two ends of an element are

for a beam $\begin{Bmatrix}V_a\\ V_b\\ M_a\\ M_b\end{Bmatrix}=\frac{2EI_b^e}{L^2}\begin{bmatrix}3 & 3\\ -3 & -3\\ 2L & L\\ L & 2L\end{bmatrix}\left\langle a_1\begin{Bmatrix}\dot{\theta}_a\\ \dot{\theta}_b\end{Bmatrix}+\begin{Bmatrix}\theta_a\\ \theta_b\end{Bmatrix}\right\rangle$ (19)

for a column

$$\begin{Bmatrix}V_a\\ V_b\\ M_a\\ M_b\end{Bmatrix}=\left\{\frac{m_c^eL}{420}\begin{bmatrix}156 & 54\\ 54 & 156\\ 156 & 54\\ 54 & 156\end{bmatrix}+\begin{bmatrix}m_a & 0\\ 0 & m_b\\ m_a & 0\\ 0 & m_b\end{bmatrix}\right\}\left\langle\begin{Bmatrix}\ddot{u}_a\\ \ddot{u}_b\end{Bmatrix}+a_0\begin{Bmatrix}\dot{u}_a\\ \dot{u}_b\end{Bmatrix}\right\rangle+\frac{2EI_c^e}{H^3}\begin{bmatrix}6 & -6 & -3H & -3H\\ & 6 & 3H & 3H\\ & & 2H^2 & H^2\\ sym & & & 2H^2\end{bmatrix}\left\langle a_1\begin{Bmatrix}\dot{u}_a\\ \dot{u}_b\\ \dot{\theta}_a\\ \dot{\theta}_b\end{Bmatrix}+\begin{Bmatrix}u_a\\ u_b\\ \theta_a\\ \theta_b\end{Bmatrix}\right\rangle \quad (20)$$

Allowing for the rotational inertia, then its shear forces and moments of an element are

for a beam $\begin{Bmatrix}V_a\\ V_b\\ M_a\\ M_b\end{Bmatrix}=\frac{m_b^eL^3}{420}\begin{bmatrix}0 & 0\\ 0 & 0\\ 4 & -3\\ -3 & 4\end{bmatrix}\left\langle\begin{Bmatrix}\ddot{\theta}_a\\ \ddot{\theta}_b\end{Bmatrix}+a_0\begin{Bmatrix}\dot{\theta}_a\\ \dot{\theta}_b\end{Bmatrix}\right\rangle+\frac{2EI_b^e}{L^2}\begin{bmatrix}3 & 3\\ -3 & -3\\ 2L & L\\ L & 2L\end{bmatrix}\left\langle a_1\begin{Bmatrix}\dot{\theta}_a\\ \dot{\theta}_b\end{Bmatrix}+\begin{Bmatrix}\theta_a\\ \theta_b\end{Bmatrix}\right\rangle$ (21)

for a column

$$\begin{Bmatrix}V_a\\ V_b\\ M_a\\ M_b\end{Bmatrix}=\frac{m_c^eL}{420}\begin{bmatrix}156 & 54 & -22L & 13L\\ & 156 & -13L & 22L\\ & & 4L^2 & -3L^2\\ sym & & & 4L^2\end{bmatrix}\left\langle\begin{Bmatrix}\ddot{u}_a\\ \ddot{u}_b\\ \ddot{\theta}_a\\ \ddot{\theta}_b\end{Bmatrix}+a_0\begin{Bmatrix}\dot{u}_a\\ \dot{u}_b\\ \dot{\theta}_a\\ \dot{\theta}_b\end{Bmatrix}\right\rangle+\frac{2EI_c^e}{H^3}\begin{bmatrix}6 & -6 & -3H & -3H\\ & 6 & 3H & 3H\\ & & 2H^2 & H^2\\ sym & & & 2H^2\end{bmatrix}\left\langle a_1\begin{Bmatrix}\dot{u}_a\\ \dot{u}_b\\ \dot{\theta}_a\\ \dot{\theta}_b\end{Bmatrix}+\begin{Bmatrix}u_a\\ u_b\\ \theta_a\\ \theta_b\end{Bmatrix}\right\rangle \quad (22)$$

II.2. THE REDUCTION OF LATERAL STIFFNESS CAUSED BY ROTATIONAL STIFFNESS

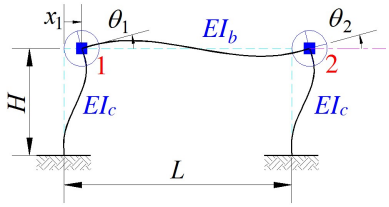

Fig. 6.: A single-portal frame

To analyze the effect of rational stiffness on lateral stiffness, consider a single-portal frame with its dimensions shown in Fig. 6. Ignoring the rotational inertia of a node and structural damping, the equation of motion (14) is rewritten as

$$\left[\begin{array}{c|c} \mathbf{M}_{n\times n} & \mathbf{0}_{n\times(m+1)} \\ \hline \mathbf{0}_{(m+1)\times n} & \mathbf{0}_{n(m+1)\times n(m+1)} \end{array}\right]\left\{\begin{array}{c} \ddot{\mathbf{x}}_{n\times 1} \\ \hline \ddot{\boldsymbol{\theta}}_{n(m+1)\times 1} \end{array}\right\}+ \left[\begin{array}{c|c} \mathbf{K}_{n\times n} & \mathbf{K}_{n\times n(m+1)} \\ \hline \mathbf{K}_{n(m+1)\times n} & \mathbf{K}_{n(m+1)\times n(m+1)} \end{array}\right]\left\{\begin{array}{c} \mathbf{x}_{n\times 1} \\ \hline \boldsymbol{\theta}_{n(m+1)\times 1} \end{array}\right\}=\left\{\begin{array}{c} \mathbf{P}_{n\times 1} \\ \hline \mathbf{0}_{n(m+1)\times 1} \end{array}\right\} \quad (23)$$

$$\text{or} \quad \begin{cases} \mathbf{M}_{n\times n}\ddot{\mathbf{x}}_{n\times 1}+\left[\mathbf{K}_{n\times n}-\mathbf{K}_{n\times n(m+1)}\mathbf{K}^{-1}_{n(m+1)\times n(m+1)}\mathbf{K}_{n(m+1)\times n}\right]\mathbf{x}_{n\times 1}=\mathbf{P}_{n\times 1} \\ \boldsymbol{\theta}_{n(m+1)\times 1}=-\mathbf{K}^{-1}_{n(m+1)\times n(m+1)}\mathbf{K}_{(m+1)\times n}\mathbf{x}_{n\times 1} \end{cases} \quad (24)$$

The equation (24) indicates that the lateral stiffness is cut by $\mathbf{K}_{n\times(m+1)}\mathbf{K}^{-1}_{n(m+1)\times n(m+1)}\mathbf{K}_{(m+1)\times n}$ compared with no consideration to rotational stiffness. For the frame in the Fig consisting of one lateral and two displacements, a global stiffness matrix having 3×3 dimension is $\mathbf{K}=\left[\begin{array}{c|cc} \frac{24EI_c}{H^3} & \frac{6EI_c}{H^2} & \frac{6EI_c}{H^2} \\ \hline \frac{6EI_c}{H^2} & \frac{4EI_c}{H}+\frac{4EI_b}{L} & \frac{2EI_b}{L} \\ \frac{6EI_c}{H^2} & \frac{2EI_b}{L} & \frac{4EI_c}{H}+\frac{4EI_b}{L} \end{array}\right]$ in which

$$\mathbf{K}_{n\times n}=\frac{24EI_c}{H^3};\ \mathbf{K}_{n\times n(m+1)}=\mathbf{K}^T_{n(m+1)\times n}=\left[\begin{array}{c|c} \frac{6EI_c}{H^2} & \frac{6EI_c}{H^2} \end{array}\right];\ \mathbf{K}_{n(m+1)\times n(m+1)}=\left[\begin{array}{c|c} \frac{4EI_c}{H}+\frac{4EI_b}{L} & \frac{2EI_b}{L} \\ \hline sym & \frac{4EI_c}{H}+\frac{4EI_b}{L} \end{array}\right]$$

And an equivalent lateral-stiffness matrix of a single portal frame is

$$\hat{\mathbf{K}}_{n\times n}=\mathbf{K}_{n\times n}-\mathbf{K}_{n\times n(m+1)}\mathbf{K}^{-1}_{n(m+1)\times n(m+1)}\mathbf{K}_{n(m+1)\times n}=\frac{12EI_c(6I_bH+I_cL)}{H^3(3I_bH+2I_cL)} \quad (25)$$

From this analysis and neglecting the rotational inertia, the equation **Error! Reference source not found.** can be rewritten in more simple matrix form as

$$\begin{cases} \mathbf{M}_{n\times n}\ddot{\mathbf{x}}_{n\times 1}+\mathbf{C}_{n\times n}\dot{\mathbf{x}}_{n\times 1}+\hat{\mathbf{K}}_{n\times n}\mathbf{x}_{n\times 1}=\mathbf{P}_{n\times 1}-\mathbf{M}_{n\times n}\mathbf{1}_{n\times 1}\ddot{x}_g-\mathbf{F}^{\mathbf{VFD}}_{n\times 1} \\ \boldsymbol{\theta}_{n(m+1)\times 1}=\left(-\mathbf{K}^{-1}_{n(m+1)\times n(m+1)}\mathbf{K}_{(m+1)\times n}\right)\mathbf{x}_{n\times 1} \end{cases} \quad (26)$$

The equation (25) has a form as a shear frame model, a system with rigid beams or no rotation at beam's ends. Correspondingly, the equation (26) is very helpful to lessen computation time cost for a frame having hundreds of nodes or in virtual of decreasing DOFs from $n(m+2)$ to n. The numerical results of the equation (14) (allowing for the rotational inertia at nodes) and (26) (neglecting the rotational inertia at nodes) are compared in the numerical example hereafter.

II.3. COMPUTATIONAL ALGORITHM FOR THE SOLUTION OF MOTION EQUATION

Due mosty to damper forces generated from VFD, the equation (14) is resolved by using the Newmark method, a numerical method modified in time domain. The time domain is given by a set of discrete values Δt which are ususally taken to be constant. The response is determined at the discrete time instants t_i. Accordingly the displacement, velocity, and acceleration of a structure at the time t_i are denoted as $u_i, \dot{u}_i, \ddot{u}_i$ respectively. The response quantities at the time instants t_{i+1} depend on not only applied loads but also the preceding quantities at the time i. In the time series data after assembling, the numerical procedures of a structure added with VFD (14) is presented in Fig. 7. This paper uses the MATLAB routine to solve the equation (14) following this flowchart. Solving the differential equation (26) is similar to (14), in which unknowns $\mathbf{u}, \dot{\mathbf{u}}, \ddot{\mathbf{u}}$ are replaced with $\mathbf{x}, \dot{\mathbf{x}}, \ddot{\mathbf{x}}$ first and unknows $\boldsymbol{\theta}$ is successively computed using $\mathbf{x}$.

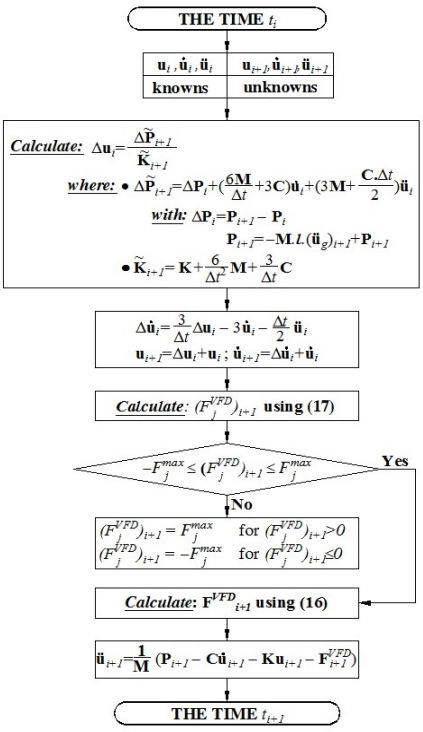

Fig. 7. Algorithm of a typical time interval (t_{i+1}-t_i)

II. NUMERICAL EXAMPLES

III.2. A NINE-STORY BUILDING OF BENCHMARK PROBLEMS

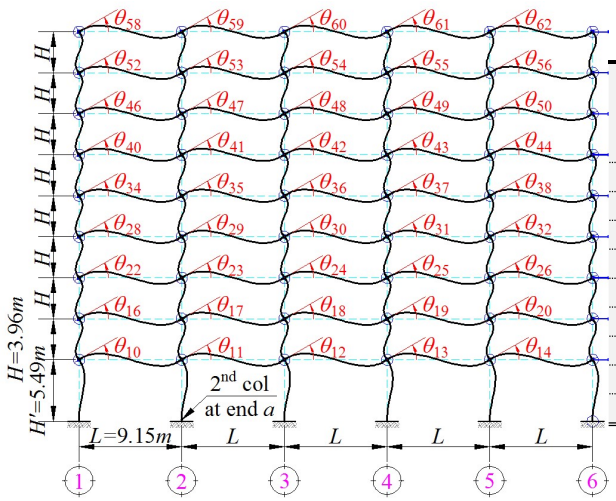

Fig. 8: A benchmark 9-story building

Table 1. The dynamic properties of the 9-story building

j^{th} floor	Column section	beam section	m_j $(\times 10^3 kg)$	$W_j = m_j g$ (kN)	floor level $Z_j(m)$
1st	W14x500	W36x160	202.0	1981.6	5.49
2nd	W14x455	W36x160	197.8	1940.4	9.45
3rd	W14x455	W36x135	197.8	1940.4	13.41
4th	W14x370	W36x135	197.8	1940.4	17.37
5th	W14x370	W36x135	197.8	1940.4	21.33
6th	W14x283	W36x135	197.8	1940.4	25.29
7th	W14x283	W30x99	197.8	1940.4	29.25
8th	W14x257	W27x84	197.8	1940.4	33.21
9th	W14x257	W24x68	214.0	2099.3	37.17

So as to demonstrate seismic response of a structure effectively controlled with VFD, the 9-story steel building, one of the benchmark problems [8], is utilized with E=2.10^4kN/cm^2, damping ratios for two first mode ζ_1=ζ_2=2%, and yield strength σ_y=345MPa. Its dynamic properties are given in Table 1. The weight at the j^{th} floor is $W_j = m_j g$ with the gravitational acceleration $g = 9.81 m/s^2$. The degree of freedoms and nodes of structure eliminated with boundary condition are n_{dof}=71 and n_{node}=54, respectively. The first three natural periods of the structure are $T_1 = 1.2865s$; $T_2 = 0.4880s$; $T_3 = 0.2839s$. The ElCentro earthquake excitation along the x axis and with peak ground acceleration (PGA) of $\left(\ddot{x}_g\right)_{\max} = 0.35g$ [3] does not include rotation acceleration about the z axis ($\ddot{\theta}_g = 0$). Analysis duration is 35 seconds or nt=28001 and time intervals Δt=0.00125 second. The response of the structure are analysized in cases as **(A)$_{NCT}$** – the non-controlled structure analyzed with SF model; **(A)$_{VFD}$** - the VFD controlled structure analyzed by using SF; **(B)$_{NCT}$** - the non-controlled structure analyzed by using GA and neglecting its rotational inertia; **(B)$_{VFD}$** - the VFD controlled structure analyzed by using (B); **C)$_{NCT}$** - the non-controlled structure analyzed with GA and allowing for its rotational inertia; **(C)$_{VFD}$** - the VFD controlled structure analyzed by using (C); **(D)$_{NCT}$** - the non-controlled structure analyzed by using SAP2000 (Structural Analysis Program) with modal response analysis. VFD controlling properties of floors are $\begin{cases} C_j^{VFD} = h.c_j \\ \alpha_j = 0.9 \\ f_{j,\max}^{VFD} = 300kN \end{cases} \left(\begin{matrix} h = 10 \\ j = \overline{1,9} \end{matrix} \right)$ with c_j are coefficients in lateral damping matrix $\mathbf{C}_{n\times n}$. Displacement and acceleration errors in (B) compared to (C) are determined as

$$error(\%) = \frac{\sum_{j=1}^{n=9} \sqrt{\frac{\sum_{t=1}^{nt=28001} \left(u_{j,t}^{(B)} - u_{j,t}^{(C)}\right)^2}{nt}}}{\sum_{j=1}^{n=9} \sqrt{\frac{\sum_{t=1}^{nt=28001} \left(u_{j,t}^{(C)}\right)^2}{nt}}} \times 100 \quad (27)$$

Table 2. Errors of the pairwise cases

	(B)$_{NCT}$ vs (C)$_{NCT}$	**(C)$_{NCT}$ vs (D)$_{NCT}$**	**(B)$_{VFD}$ vs (C)$_{VFD}$**
Displacement	1.39%	3.40%	1.02%
Acceleration	7.35%	17.27%	1.88%

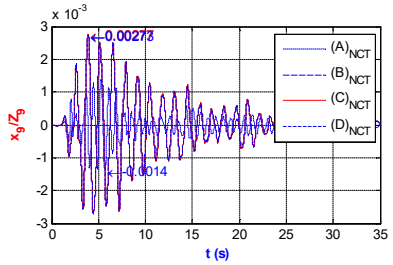

Fig. 9. Story drift response without VFD

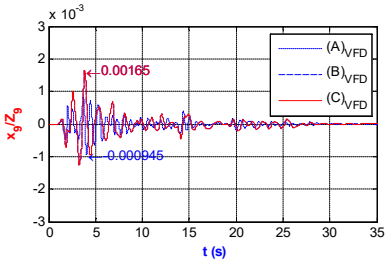

Fig. 10: Story drift response with VFD

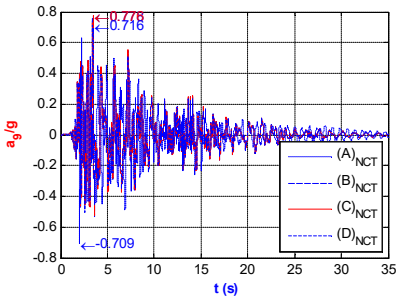

Fig. 11: Top acceleration response without VFD

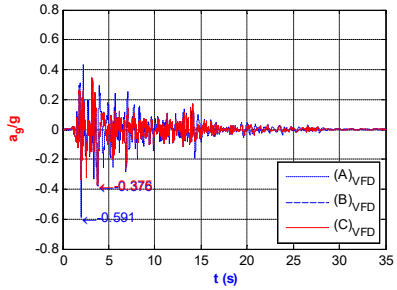

Fig. 12. Top acceleration response with VFD

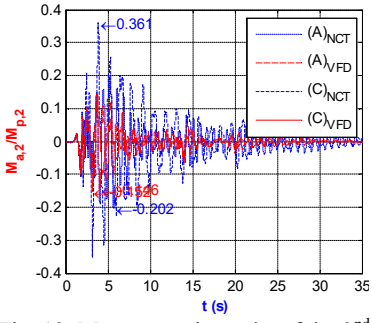

Fig. 13. Moment at the end a of the 2nd column

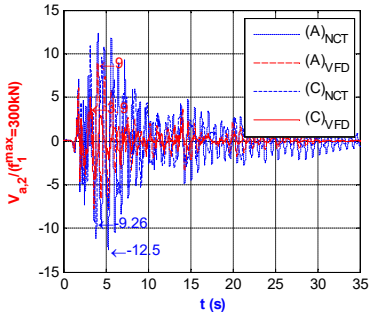

Fig. 14. Shear force at the end a of the 2nd column

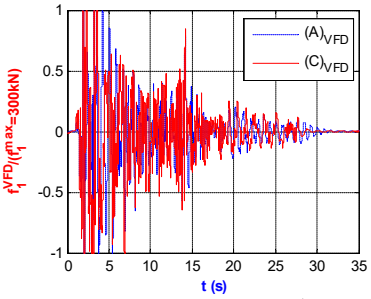

Fig. 15. VFD force of the 1st story

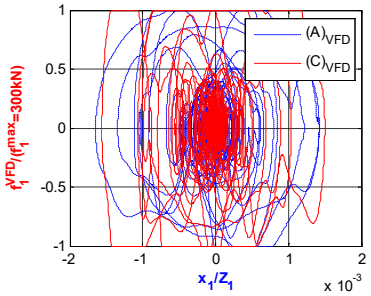

Fig. 16. Hysteretic loop

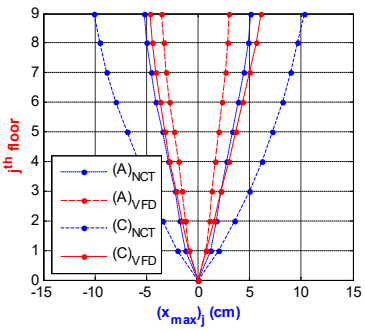

Fig. 17. Maximum story drift

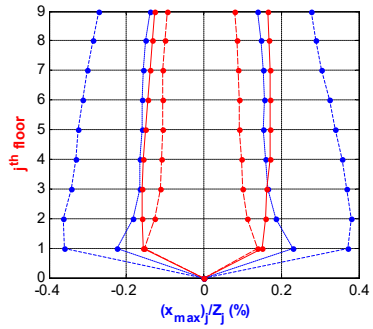

Fig. 18. Ratio of maximun story drift to its height

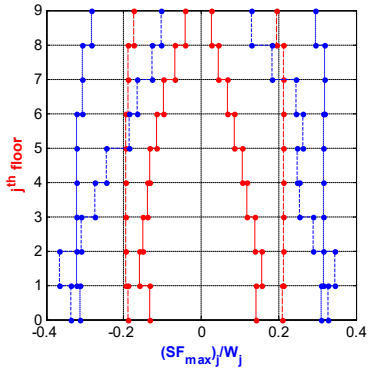

Fig. 19. Ratio of columns' maximum shear forces at 2-axis to its weight

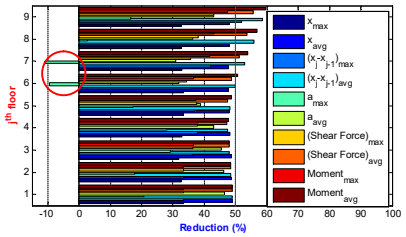

Fig. 20. Dynamic reduction using the case $(A)_{VFD}$ (α_j=0.9)

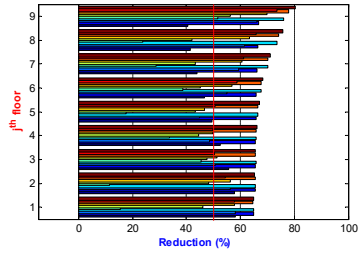

Fig. 21.Dynamic reduction using the case $(C)_{VFD}$ (α_j=0.9)

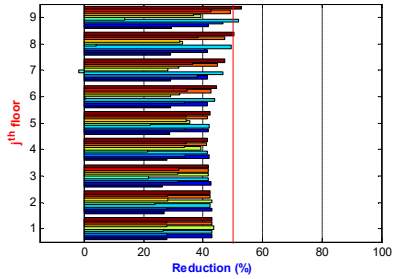

Fig. 22. Dynamic reduction using the case $(A)_{VFD}$ (α_j=1.0)

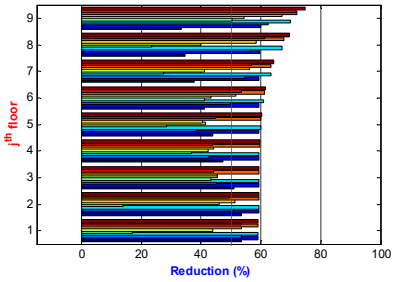

Fig. 23. Dynamic reduction using the case $(C)_{VFD}$ (α_j=1.0)

The reliable numerical method proposed in the paper is illustrated according to Table 2 and Fig. 9, Fig. 10, Fig. 11, and Fig. 12. Displacement and acceleration errors in pairwise cases (B) and (C) are insignificant, that is, kinetic energy of rotational motion slightly contributes to kinetic energy of the system. Therefore, (B) rather than (C) is used for dynamic analysis of a VFD structure in efforts to reduce amounts of computation in the proposed numerical method. Displacement error of pairwise cases (C) and (D) is unimportant while acceleration error reaches 17.3%. The leading cause is that (C) uses linear acceleration approximated in Time-NewMark Method while (D) uses Modal Response analysis. Because column moment M at the 1st floor is completely lower than plastic moment M_p (Fig. 13) and story drift $x_9 / Z_9 < 1/300$ [9], the first-order analysis in proposed theorical model is acceptable.

With respect to (A), the lateral stiffness of the 9-story structure results from the lateral stiffness of the columns and is not diminished by beams' flexural stiffness. Hence, the structure in (A) is stiffer and its lateral displacements is always lower and its lateral accelerations is greater than in (C).

In (C) the structure added with VFD using ratio of only $f^{VFD} / f^{VFD}_{\max} = 1$ compared to $SF / f^{VFD}_{\max} = 9.26$ has got the maximum displacement reduction of 58%, thanks to increasing lateral force resistance for structures. This result demonstrates the capacity of response reduction for structures retrofitted with VFD. Furthermore, VFD capacity is higher in a case of decreasing α (Fig. 21 and Fig. 23). $(C)_{VFD}$ is more sophisticated method than $(A)_{VFD}$ and therefore give higher reliability of VFD usefulness.

Analyzing results show that decreasing α is the cause of increasing acceleration response or negative reduction (Fig. 20 at the 6th and 7th floors). The more effective in reducing response is obtained as higher $f^{VFD}_{\max}$, thanks to bigger hysteretic loop (Fg. 16).

IV. CONCLUSION

This paper explores the dynamic behavior of structures fitted with Viscous Fluid Dampers (VFD) with the goal of withstanding seismic loads. A computational model, along with a modified Time-NewMark algorithm, is introduced to determine the dynamic behaviors of structures equipped with VFD. Two steel structures are used in the numerical example to validate the proposed numerical method and compare their dynamic responses using three different approaches: (1) Shear Frame model, (2) General Approach model that either disregards or accounts for rotational inertia, and (3) Finite Element model using the Structural Analysis Program 2000. In the General Approach, treating slabs, not beams, as rigid bodies results in more accurate dynamic responses than in the Shear Frame model, leading to a more precise evaluation of the effectiveness of the VFD structure. When structures are subjected to more intense seismic excitation, the maximum damping force in the VFD should be increased to achieve the desired reduction, rather than adjusting their damping coefficient and exponential parameters.

REFERENCES

[1] Bathe, K.-J., Finite Element Procedures in Engineering Analysis, Prentice Hall, Englewood Cliffs, NJ., 1982
[2] Anil K. Chopra (2012), "Dynamics of Structures", 4th edition, Prentice Hall Press.
[3] http://www.vibrationdata.com
[4] Robert J. McNamara and Douglas P. Taylor (2003), "Fluid viscous dampers for high-rise buildings", the structural design of tall and special buildings, Vol.12, pp.145–154, http://taylordevices.com/literature.html
[5] Douglas P. Taylor, Israel Katz (2004) – Seismic protection with fluid viscous dampers for the Torre Mayor, a 57 story office tower in Mexico City, Mexico, http://taylordevices.com/literature.html
[6] M.C. Constantinou, M.D. Symans (1993), "Experimental study of seismic response of buildings with supplemental fluid dampers", The structural Design of tall buildings, pp. 93-132.
[7] M. Ahmadizadeh, "Equivalent passive systems for semi-active viscous fluid dampers", 4th World Conference on Structural Control and Monitoring.
[8] Y.Ohtori, R. E. Christenson, B. F. Spencer (2004), "Benchmark Control Problems for Seismically Excited Nonlinear Buildings", Journal of Engineering Mechanics © ASCE / April 2004.
[9] TCXDVN 338:2005 about Steel Structure - Design Standard, http://www.xaydung.gov.vn/web/guest/english